

DEVELOPMENT OF MULTI-WAVELENGTH HIGH-SPECTRAL-RESOLUTION LIDAR SYSTEM ($2\alpha+3\beta+2\delta$)

Tomoaki Nishizawa, Nobuo Sugimoto, and Ichiro Matsui

National Institute for Environmental Studies, 16-2 Onogawa, Tsukuba, 305-0052, Japan,
nisizawa@nies.go.jp

ABSTRACT

A multi-wavelength High-Spectral-Resolution Lidar (HSRL) system for the next-generation lidar network is being developed. This lidar system provides $2\alpha+3\beta+2\delta$ data: extinction coefficients (α) at 355 and 532 nm, backscatter coefficients (β) at 355, 532, and 1064 nm, and depolarization ratios (δ) at 532 and 1064 nm. This system combines use of the previously developed HSRL techniques with an iodine absorption filter for 532nm and a Fabry-Perot etalon for 355nm. We constructed the 532nm HSRL and 1064nm receiver systems of this lidar. We also developed a system to tune the laser wavelength to an iodine absorption line in this lidar system and conducted preliminary measurements using the constructed systems. The temporal and vertical variation of aerosols could be determined. The constructed 532nm HSRL system could measure molecule Rayleigh backscatter signals by blocking aerosol Mie backscatter signals with the iodine absorption filter, indicating that the developed laser wavelength tuning system worked well. Thus, we reached to the preliminary conclusion that we could construct appropriate the 532nm HSRL and 1064nm receiver systems.

1. INTRODUCTION

The National Institute for Environmental Studies (NIES) have established a ground-based lidar network (NIES lidar network) covering a wide area in East Asia since 2001 in order to monitor and understand the movements and the optical properties of Asian dust and air-pollution aerosols [1,2]. A compact two-wavelength (532 and 1064nm) backscatter (β) and one-wavelength (532nm) polarization (δ) Mie-scattering lidar system (i.e., $2\beta+1\delta$ lidar system) with automatic measurement capability is used in the network observation.

To better understand the optical properties as well as the movements of Asian dust and air-pollution aerosols, we decided to develop a multi-channel lidar system using High-Spectral Resolution Lidar (HSRL) techniques for the next-generation NIES lidar network [3]. The developed lidar system provides $2\alpha+3\beta+2\delta$ data (i.e., extinction coefficient (α) at 355

and 532 nm; backscatter coefficient (β) at 355, 532, and 1064 nm; and depolarization ratio (δ) at 532 and 1064 nm [4]). We use a 532nm HSRL technique with an iodine filter developed at NIES [5,6] and a 355nm HSRL technique using a Fabry-Perot etalon developed at the University of Fukui [7]. We further seek to develop a compact lidar system with automatic measurement capability to realize temporally continuous measurements day and night and network measurements like the NIES lidar network and MPLNET [8].

The key features of the developed lidar system are 1) independent extinction measurement, 2) multichannel measurement, and 3) a highly sensitive method. The independent extinction and multichannel measurements can provide useful data for characterizing aerosol optical properties as demonstrated by multichannel Raman lidar measurements in EARLINET [e.g., 9]. Furthermore, the independent, multichannel measurements are essential for classifying aerosol components such as dust, sea-salt, and black-carbon and for estimating their optical properties [10,11]. We have proposed an algorithm to classify dust, sea-salt, black-carbon, and water-soluble particles and to retrieve their extinction coefficients and particle sizes using the developed lidar data (i.e., $2\alpha+3\beta+2\delta$ data) [3]. HSRL is a highly sensitive method and helps us to measure signals with sufficient signal-to-noise ratio in daytime as well as nighttime.

In this paper, we report the latest status of this lidar system development. We have completed constructing the 532nm HSRL and 1064nm receiver systems of this lidar. We introduce their systems (section 2) and present data actually measured with their systems (section 3).

2. MULTI-WAVELENGTH HSRL SYSTEM

The configuration and specifications of the developed lidar system are presented in Fig. 1 and Table 1. The design and the key techniques of this lidar system have been described in [4] in detail. Here, we outline the lidar system.

The developed lidar employs a commercial compact injection seeded Nd:YAG laser with second- and

third-harmonics generators. The injection seeder uses a fiber laser; the temperature control of the fiber laser is essential. The coaxial transmitted and received beams are reflected vertically with a large mirror. Backscattered light is collected with a horizontally mounted telescope. The collected light is split into the three receivers at 1064, 532, and 355nm using dichroic beam splitters. The receiver systems are built on the first level for 1064 and 532nm and on the second level for 355nm; the received 355nm signal is transferred to second level using an optical fiber.

At 1064nm, parallel and perpendicular polarization components of the total (Mie+Rayleigh) scattering are detected with two APDs (APD_{1064,||} and APD_{1064,⊥}). At 532nm, the molecule Rayleigh backscatter signals are detected with a PMT (PMT_{532,Ray}) after the temperature-controlled 40cm iodine absorption filter blocks particle Mie backscatter signals. The parallel and perpendicular polarization components of the total backscatter are detected with two PMTs (PMT_{532,||} and PMT_{532,⊥}). At 355nm, the particle Mie backscatter signals are detected with two PMTs (PMT_{355,Mie,ch1} and PMT_{355,Mie,ch2}) after the pressure- and temperature-controlled Fabry-Perot etalon transmits the particle Mie backscatter signals (blocks the molecule backscatter). The total backscatter is also detected with a PMT (PMT₃₅₅). To evaluate the HSRL measurement at 355nm, a 387nm N₂ Raman scatter receiver (PMT_{387,Raman}) is set on the first level.

To use a single laser, we tune the second harmonic of the laser to an iodine absorption line, and then tune the Fabry-Perot etalon to the third harmonic of the laser. A tuning method using an iodine filter and an acoustic-optic modulator (AOM) was developed in the previous study [5]. This method uses the zeroth-order and first-order beams from the AOM, using a small portion of the transmitted laser separated with a partial mirror. We improve this method by using +first-order and -first-order beams from two AOMs, in order to more sensitively detect the laser frequency variation and its direction. This laser wavelength tuning system is constructed on the first level. The wavelength of the etalon is tuned by balancing Mie backscatter signals detected by the two PMTs (i.e., PMT_{355,Mie,ch1} and PMT_{355,Mie,ch2}). The output of the etalon is focused with a lens with a 1m focal length; the diameter of the focused light becomes 4mm. A mirror with a small hole of 3mm in diameter at its center is set at the focal point. The PMT_{355,Mie,ch1} detects the focused light passing through the hole of the mirror, and the PMT_{355,Mie,ch2} detects the light reflected by the mirror. We confirmed by numerical simulation that the wavelength of the etalon could be tuned using the signals of the two PMTs [4].

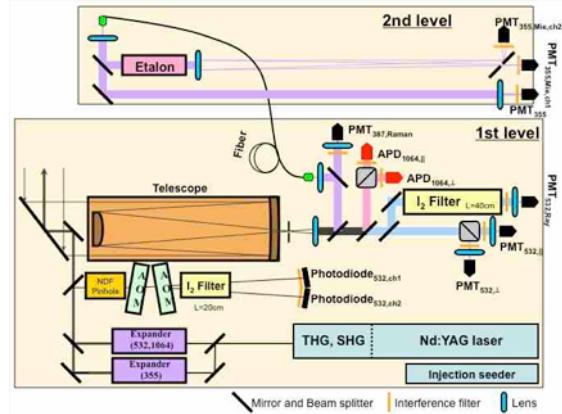


Fig. 1. Lidar system configuration. This lidar system consists of two layers: the transmitter, telescope, 532nm HSRL, 1064nm receiver, and the laser wavelength tuning system are built on the bottom layer (first level). The 355nm HSRL system is built on the top layer (second level).

Table 1. Lidar system specifications.

Transmitter	
Laser type	Nd:YAG, Q-switched, injection-seeded, linearly polarized (Continuum Surelite I)
Wavelength	1064, 532, 355nm
Line width	0.005cm ⁻¹
Pulse energy	100mJ for each wavelengths
Repetition rate	10Hz
Divergence	0.1mrad (using a 5x expander)
Receiver	
Telescope	Cassegrain, D=21cm
FOV	0.5mrad
Detectors	<ul style="list-style-type: none"> Licel APD for 1064nm Licel PMT for 532, 355nm Licel PMT for 387nm (N₂ Raman channel)
Detections and wavelength separators	
Interference filter	1nm (FWHM) for each wavelength
Rayleigh, 532nm	40cm iodine cell
Mie, 355nm	Fabry-Perot etalon (Finesse =10, FSR=5GHz)
Data acquisition	
	<ul style="list-style-type: none"> A/D converter for 532, 1064nm (25MHz, 12bit) Licel transient recorder for 355, 387nm (40MHz, 12bit)

3. 532nm HSRL and 1064nm RECEIVER SYSTEMS

We started developing this multi-channel HSRL system in 2008 as a three-year project. We have so far finished constructing the transmitter, 532nm HSRL, 1064nm receiver, and the laser wavelength tuning system on the first level (Fig. 2).

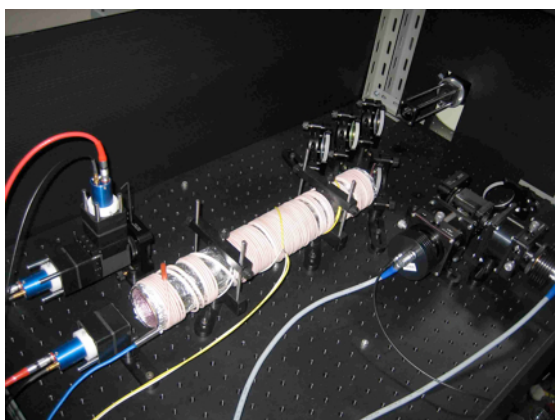


Fig. 2. Photographs of the lidar system. Upper figure: Transmitter, and laser wavelength tuning system (in the black box at the center of the photograph). Lower figure: 532nm HSRL and 1064nm receiver. The lidar system is built in a small container (W2m×L4m×H2m).

We started measurements using the constructed systems to check their performance. The signals were measured with 6m vertical resolution and 10s temporal resolution (100 shots). We averaged the raw data every 180m and 30min (18,000shots). The averaged data were used in the following discussion. Examples of the measured data are presented in Fig. 3. Clear-sky conditions prevailed for the measurements. The measured signals of the 1064nm total backscatter, the co-polar and cross-polar components of the 532nm total backscatter below 5km suddenly increased after 1600LT, indicating that dust had appeared. In contrast, the signals measured with the $\text{PMT}_{532,\text{Ray}}$ (Fig. 1) do not increase but rather decrease after 1600LT. The vertical profiles of the $\text{PMT}_{532,\text{Ray}}$ in high altitudes roughly match the vertical profiles of molecule backscatter signals simulated using a standard atmosphere profile [12] (Fig. 4). These results indicate that the iodine filter could block the aerosol Mie backscatter signals appropriately and that we could tune the laser wavelength to the iodine absorption line. During the observation, we checked the frequency variation of the laser by monitoring two signals measured with two photodiodes in the laser wavelength tuning system (Photodiode_{532,ch1} and Photodiode_{532,ch2} in Fig. 1).

We confirmed that the frequency variation of the laser was rather smaller ($\pm 0.3\text{pm}$) than the line width of the iodine absorption line used in this study (more than 2pm FWHM).

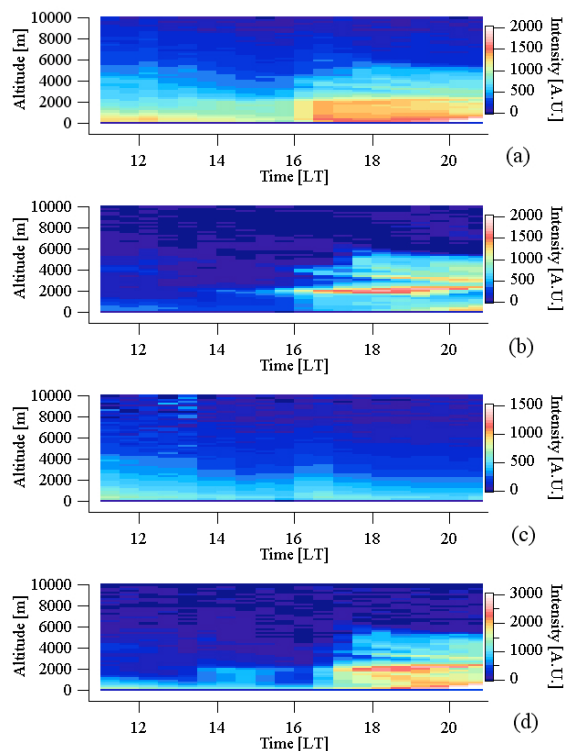


Fig. 3. Time-height cross sections of range-corrected signals measured with (a) $\text{PMT}_{532,\parallel}$ (co-polar component of the 532nm total backscatter), (b) $\text{PMT}_{532,\perp}$ (cross-polar component of the 532nm total backscatter), (c) $\text{PMT}_{532,\text{Ray}}$ (532nm Rayleigh backscatter), and (d) APD_{1064} (1064nm total backscatter) from 1100 to 2100 LT on March 11, 2010, in Tsukuba (140.12E, 36.05N), Japan.

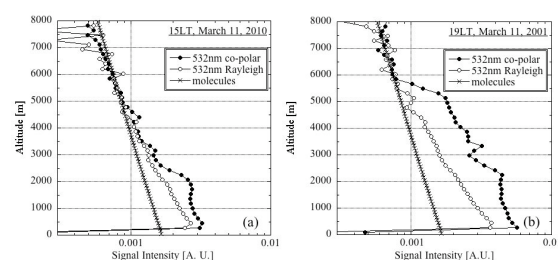


Fig. 4. Vertical profiles of range-corrected signals measured with the $\text{PMT}_{532,\parallel}$ (532nm co-polar) and $\text{PMT}_{532,\text{Ray}}$ (532nm Rayleigh) (a) at 1500LT and (b) 1900LT on March 11, 2010, in Tsukuba (140.12E, 36.05N), Japan. The vertical profiles of molecule backscatter signals (molecules) are computed using a standard atmosphere profile [12].

The data quality for the 532nm Rayleigh backscatter signals measured with the $\text{PMT}_{532,\text{Ray}}$ seems to be somewhat better for nighttime than for daytime; the

SN ratios at 2 and 4km are 100 and 10 for daytime and 200 and 30 for nighttime. More observation is needed to check the data quality.

4. CONCLUSION AND FUTURE PLAN

A multi-wavelength HSRL system ($2\alpha+3\beta+2\delta$) is being developed for the next-generation lidar network. We finished constructing the transmitter, 532nm HSRL, 1064nm receiver, and laser wavelength tuning system. We conducted half-day measurements using the constructed systems and confirmed that the systems worked well.

We plan the following for future lidar development.

1) We will develop an application to automatically tune the laser wavelength to the iodine absorption line during the measurement using the developed laser wavelength tuning system, to realize long-term, continuous measurements.

2) We started constructing the 355nm HSRL system (Fig. 5). In this 355nm HSRL system, we use a fiber-scrambler technique [7] to scramble the angular dependence of the received light from the different heights, using the optical fiber to transfer the 355nm received light to the second level. We will check the performance of the fiber scrambler.

3) A data analysis algorithm to derive the extinction coefficient, backscatter coefficient, and depolarization ratio for aerosols and clouds will be developed in the near future. Furthermore, we will develop an aerosol classification and retrieval algorithm using the derived $2\alpha+3\beta+2\delta$ data [3].

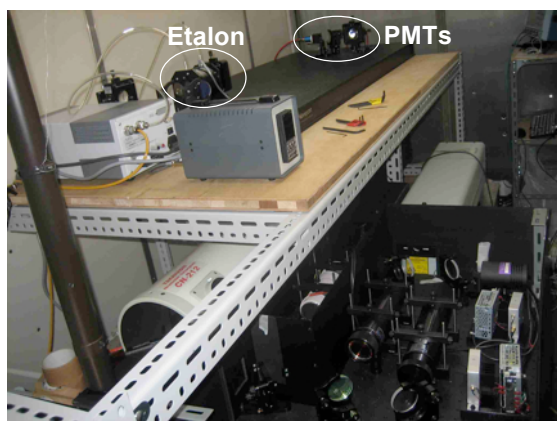


Fig. 5. Photograph of the latest lidar system. The 355nm HSRL system is on the second level (under construction).

ACKNOWLEDGEMENT

This work is supported by the Environmental Research and Technology Development Fund of the Ministry of the Environment in Japan as a three-year project starting from 2008.

REFERENCES

1. Sugimoto, N., et al., 2005: Study of Dust Transport Using a Network of Continuously Operated Polarization Lidars, *Water, Air, and Soil Pollution: Focus*, **5**, 145-157.
2. Shimizu, A., et al., 2008: NIES lidar network; strategies and applications, *Proc. 24th ILRC*, 707-710.
3. Nishizawa, T., N. Sugimoto, and I. Matsui, 2008: Development of multi-wavelength high-spectral resolution lidar and application of spheroid models to aerosol retrieval from lidar measurements, *Proc. 24th ILRC*, 361-364.
4. Sugimoto, N., et al., 2008: Multi-wavelength high-spectral resolution lidar ($2\alpha+3\beta+2\delta$) for the next generation lidar network, *Proc. 24th ILRC*, 192-195.
5. Liu, Z., I Matsui, and N. Sugimoto, 1999: High-spectral-resolution lidar using an iodine absorption filter for atmospheric measurements, *Opt. Eng.*, **38**, 1661-1670.
6. Tatarov, B., et al., 2006: Two-year-observations of optical properties of the tropospheric aerosol and clouds by a High-Spectral-Resolution Lidar over Tsukuba, Japan, *Proc. 23rd ILRC*, 451-454.
7. Imaki, M., et al., 2005: Ultraviolet high-spectral-resolution lidar using Fabry-Perot filter for the accurate measurement of extinction and lidar ratio, *Jpn. J. App. Phys.*, **44**, 3063-3067.
8. Welton, E. J., et al., 2001: Global monitoring of clouds and aerosols using a network of micro-pulse lidar systems, *Proc. Internat. Soc. Opt. Eng.*, 4153, 151-158.
9. Bösenberg, J., et al., 2003: A European Aerosol Research Lidar Network to establish an aerosol climatology, *MPI-Report 348*, Max-Planck-Institut für Meteorologie, Hamburg.
10. Nishizawa, T., et al., 2008: Algorithm to retrieve aerosol optical properties from high-spectral-resolution lidar and polarization Mie-scattering lidar measurements, *IEEE Trans. Geos. Rem. Sens.*, **46**, 4094-4103.
11. Müller, D., et al., 2007: Aerosol-type-dependent lidar ratios observed with Raman lidar, *J. Geophys. Res.*, **112**, D16202, doi: 10.1029/2006JD008292.
12. McClatchey, R. A., et al., 1972: Optical properties of the atmosphere (3rd edition), *AFCRL Environ. Res. Pap.*, 411, 108 pp.